Geophysical Journal International

Geophys. J. Int. (2015) **201,** 1814–1833 doi: 10.1093/gji/ggv065
GJI Geodynamics and tectonics

A missing-link in the tectonic configuration of the Almacık Block along the North Anatolian Fault Zone (NW Turkey): Active faulting in the Bolu plain based on seismic reflection studies

Gürol Seyitoğlu,[1] Berkan Ecevitoğlu,[2] Bülent Kaypak,[3] Korhan Esat,[1] Ayşe Çağlayan,[1] Oğuz Gündoğdu,[4] Yücel Güney,[2] Veysel Işık,[1] Emrah Pekkan,[2] Muammer Tün[2] and Uğur Avdan[2]

[1]*Department of Geological Engineering, Tectonics Research Group, Ankara University, Ankara, Turkey. E-mail: seyitoglu@ankara.edu.tr*
[2]*Earth and Space Sciences Research Institute, Anadolu University, Eskişehir, Turkey*
[3]*Department of Geophysical Engineering, Ankara University, Ankara, Turkey*
[4]*Department of Geophysical Engineering, Istanbul University, Istanbul, Turkey*

Accepted 2015 February 9. Received 2015 February 6; in original form 2014 August 30

SUMMARY

The North Anatolian Fault Zone (NAFZ) starts to branch off in the western Bolu plain. The branches of the NAFZ in this location create the Almacık block which is surrounded by the latest surface ruptures of significant earthquakes that occurred between 1944 and 1999, but its northeastern part remains unruptured. The most recently formed rupture, that was a result of the 1999 November 12 Düzce earthquake, ended to the northwest of the Bakacak Fault. The connection between the Bakacak Fault and the main branch of the NAFZ via the Bolu plain has until now remained unknown. This paper establishes that the route of the missing link runs through the Dağkent, Kasaplar and Bürnük faults, a finding achieved with the help of seismic reflection studies. The paper also argues that the cross cutting nature of these newly determined faults and a stress analysis based on focal mechanism solutions of recent earthquakes demonstrate the termination of the suggested pull-apart nature of the Bolu plain.

Key words: Earthquake interaction forecasting and prediction; Seismicity and tectonics; Continental tectonics: strike-slip and transform; Neotectonics.

1 INTRODUCTION

The North Anatolian Fault Zone (NAFZ) is located between Karlıova to the east and the Gulf of Saros to the west (Fig. 1, inset) and it stretches over 1200 km. It is a well-known, active, right-lateral, strike-slip fault zone that produces significant earthquakes (Şengör 1979; Barka & Kadinsky-Cade 1988; Barka 1992; Şengör *et al.* 2005). The eastern sector of the fault zone generally follows a narrow corridor but the western sector shows a wider shear zone composed of several branches (Barka & Kadinsky-Cade 1988; Şengör *et al.* 2005). The NAFZ starts to bifurcate in the Bolu plain. Here, its northern branch follows a route through Bolu, Düzce, Sapanca, the Gulf of İzmit, the Marmara Sea, Ganos Mountain and the Gulf of Saros. The middle branch can be traced through Abant, the Pamukova-Gevye Plain, İznik Lake, the Gulf of Gemlik and Bandırma. Some researchers, however, consider that the main fault runs through Bolu, Abant, Sapanca and the Marmara Sea. The southern branch is separated from the middle branch and follows the Yenişehir Basin and Bursa continuing south of Lakes Ulubat and Manyas (Fig. 1 and references therein).

To the west of the location where the NAFZ starts to bifurcate is a structure called the Almacık block (Şengör *et al.* 1985). Palaeomagnetic studies have suggested that the structure has rotated clockwise in between two right-lateral fault segments (Sarıbudak *et al.* 1990; Michel *et al.* 1995; İşseven *et al.* 2009). Contrary to this, a recent study has suggested anticlockwise rotations resulting from a right-lateral motion between the Armutlu peninsula and the Almacık block (Hisarlı *et al.* 2011).

The surface ruptures caused by earthquakes of 1944 February 01 Gerede ($M = 7.2$); 1957 May 26 Abant ($M = 7.1$); 1967 July 22 Mudurnu ($M = 7.2$); 1999 August 17 Kocaeli ($M = 7.4$) and 1999 November 12 Düzce ($M = 7.2$) indicate that the Almacık block is surrounded by active strike-slip faults. As shown in Fig. 2, its shape resembles a wooden shuttle as used in the textile industry. It has been suggested that the next earthquake in the region will be to the east of the 1999 November 12 Düzce earthquake rupture (Seyitoğlu 2000; Fig. 2). The epicentral distribution of the 1999 August 17 Kocaeli earthquake and its aftershocks show that the far eastern-most seismic event nearly marked the end of the following surface rupture of 1999 November 12 Düzce earthquake (Figs 3a and b). When we examine the epicentral distribution of the earthquakes after the 1999 November 12 event, the far eastern-most seismic event nearly indicates the eastern tip of the Almacık block (Fig. 3b). For this reason, it can be speculated that a future earthquake may

© The Authors 2015. Published by Oxford University Press on behalf of The Royal Astronomical Society.

Downloaded from https://academic.oup.com/gji/article/201/3/1814/754781 by ANKARA user on 12 December 2021

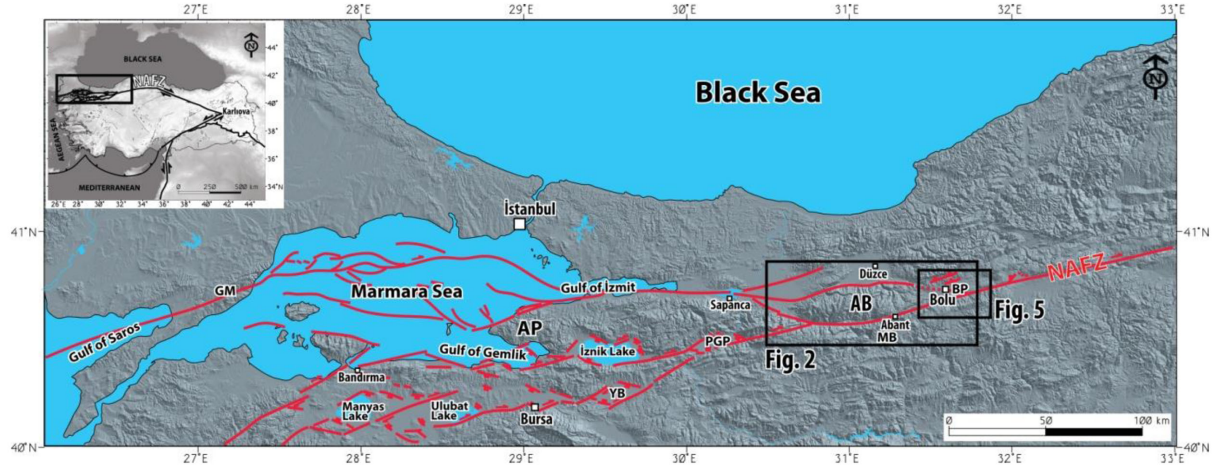


Figure 1. The North Anatolian Fault Zone (NAFZ) in the NW of Turkey. AB: Almacık Block, BP: Bolu Plain, MB: Mudurnu Basin, PGP: Pamukova-Gevye Plain, YB: Yenişehir Basin, AP: Armutlu Peninsula, GM: Ganos Mountain (Fault lines after Şengör 1979; Seyitoğlu 1984; Barka & Kadinsky-Cade 1988; Koçyiğit 1988; Barka & Kuşçu 1996; Emre *et al.* 1997; Okay *et al.* 1999; Tur *et al.* 2000; Alpar & Yaltırak 2002; Armijo *et al.* 2002; Yaltırak 2002; Herece & Akay 2003; Arca 2004; Şengör *et al.* 2005; Selim *et al.* 2006; Kurtuluş & Canbay 2007; Dolu *et al.* 2007; Yılmaz & Koral 2007; Gürbüz & Gürer 2008; Öztürk *et al.* 2009; Ayhan & Koçyiğit 2010; Bécel *et al.* 2010; Gökten *et al.* 2011).

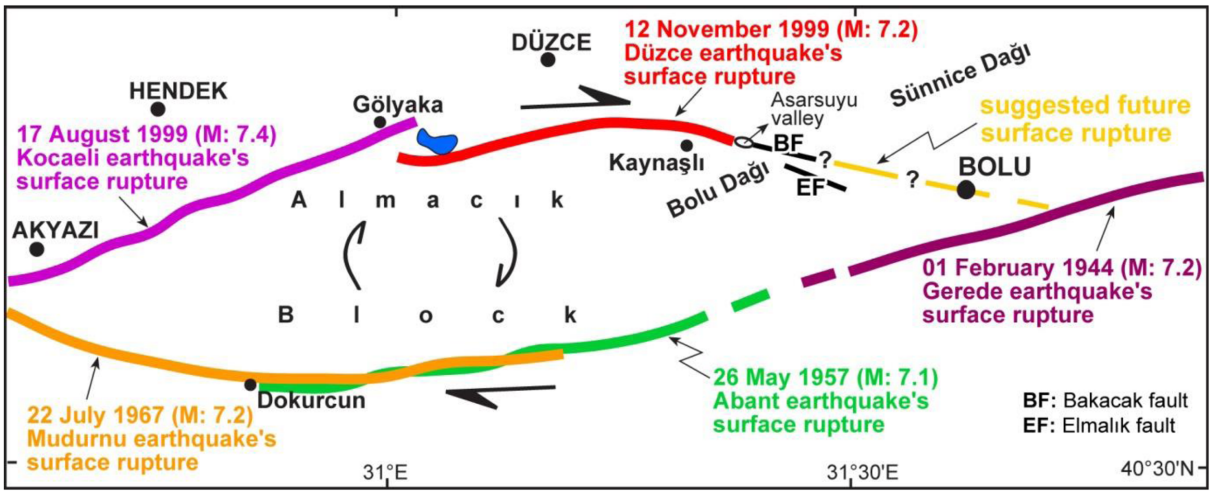


Figure 2. Surface ruptures of recent earthquakes and the Almacık block (after Seyitoğlu 2000). Bakacak and Elmalık faults after Hitchcock *et al.* (2003). For location see Fig. 1.

be expected on the recently unruptured portion of the Almacık block (Fig. 2). In order to check this hypothesis, a series of seismic reflection studies were performed in the Bolu plain and the results are presented in this paper.

2 NEOTECTONIC FRAMEWORK OF THE BOLU PLAIN

2.1 Previous work

The neotectonic features of the Bolu area were examined by Öztürk *et al.* (1985), who published a geological map and determined individual fault segments with a special emphasis on the 1944 Gerede earthquake's surface rupture (Fig. 4a). This rupture has also been recently mapped by Emre *et al.* (2011; Fig. 4b). Aktimur *et al.* (1986) provided the locations of active faults and the distribution details of Quaternary deposits in the Bolu plain (Fig. 4c). The common point of Öztürk *et al.* (1985) and Aktimur *et al.* (1986) is the NE–SW trending fault lines in the Bolu plain that lie subparallel to the 1944 surface rupture (Figs 4a and c). There are different structural evaluations of the Bolu plain and the surrounding region: while the development of the Adapazarı, Düzce and Bolu basins has been explained by a bending of the NAFZ (Neugebauer 1995), the Bolu Basin has been evaluated as a pull-apart system (Özden *et al.* 2008; Gökten *et al.* 2011; Fig. 4d). The structural analyses of fault-slip data and focal mechanism solutions around the Bolu Basin indicate that NW-trending σ_1 and NE-trending σ_3 axes are produced by a right-lateral motion of the NAFZ and a younger transtensional stress regime overprinting the earlier transpression, is attributed to the pull-apart nature of the Bolu Basin (Özden *et al.* 2008). Gökten *et al.* (2011) supported this by publishing their view of NW–SE trending normal faults in the western part of the Bolu plain (Fig. 4d). Morphology-dependent geological studies (Öztürk *et al.* 1985; Aktimur *et al.* 1986; Gökten *et al.* 2011) have generally defined the border faults of the Quaternary Bolu Basin and assume

Downloaded from https://academic.oup.com/gji/article/201/3/1814/754781 by ANKARA user on 12 December 2021

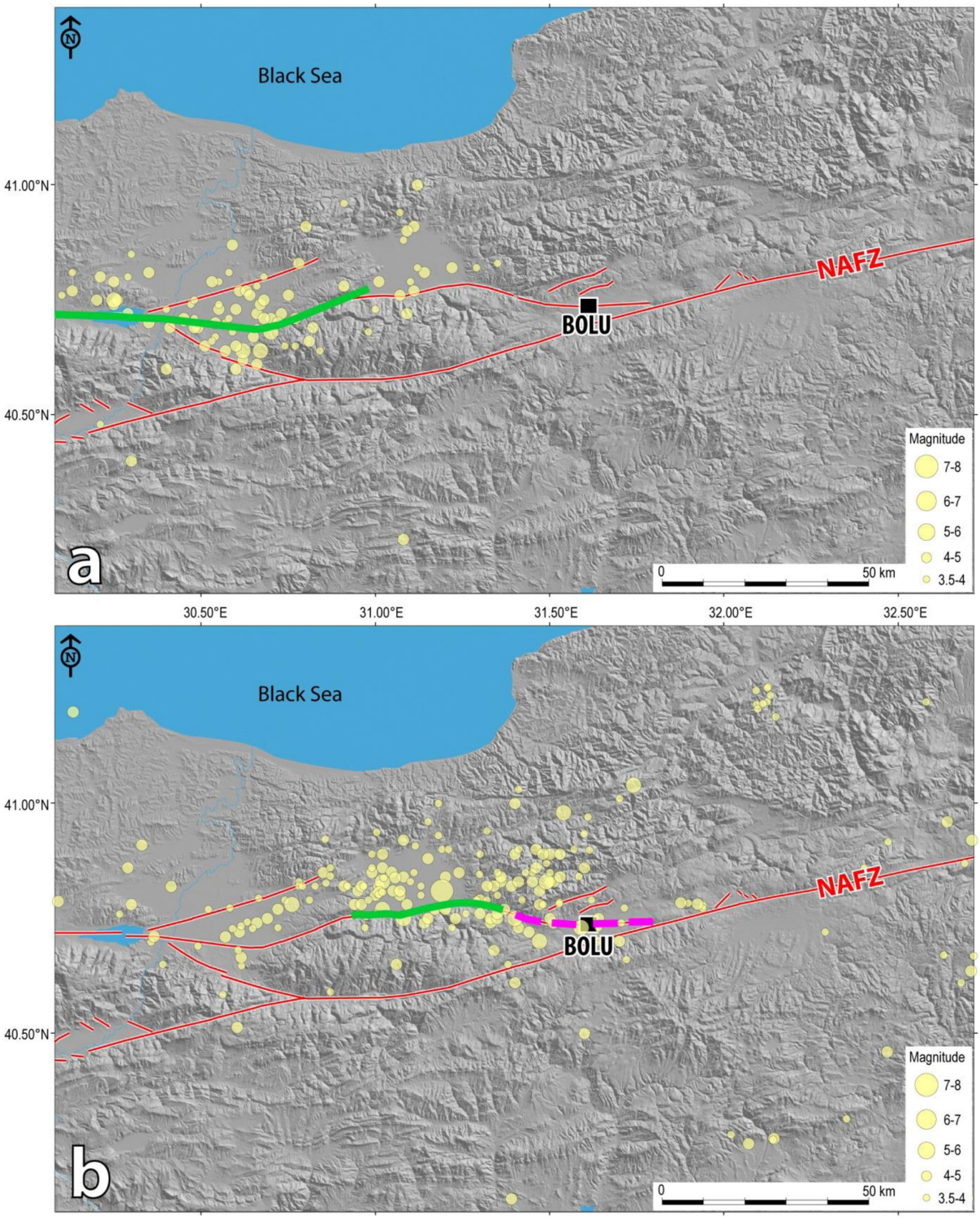


Figure 3. (a) Eastern sector of the 1999 August 17 Kocaeli earthquake surface rupture and its aftershocks. (b) The epicentre distribution of the aftershocks following the 1999 November 12 earthquake and recent seismicity in the Bolu plain. Data are from the KOERI.

that they are active. Yoshioka (1996) and Gürbüz & Gürer (2009), however, examined many pull-apart structures along the NAFZ and concluded that the active fault branch generally crosses over the pull-apart structures.

The surface rupture of the 1999 November 12 Düzce earthquake along the Düzce Fault follows an eastward direction down to the Asarsuyu valley (Fig. 2). The GPS and Insar data suggest a longer rupture towards the east than that observed in the field (Çakır *et al.* 2003). The connection of this fault to the main strand of the NAFZ, following the trace of the 1944 Gerede earthquake, is a major question as indicated by Seyitoğlu (2000). Hitchcock *et al.* (2003) closely examined the area between the Asarsuyu valley and the Bolu plain.

Downloaded from https://academic.oup.com/gji/article/201/3/1814/754781 by ANKARA user on 12 December 2021

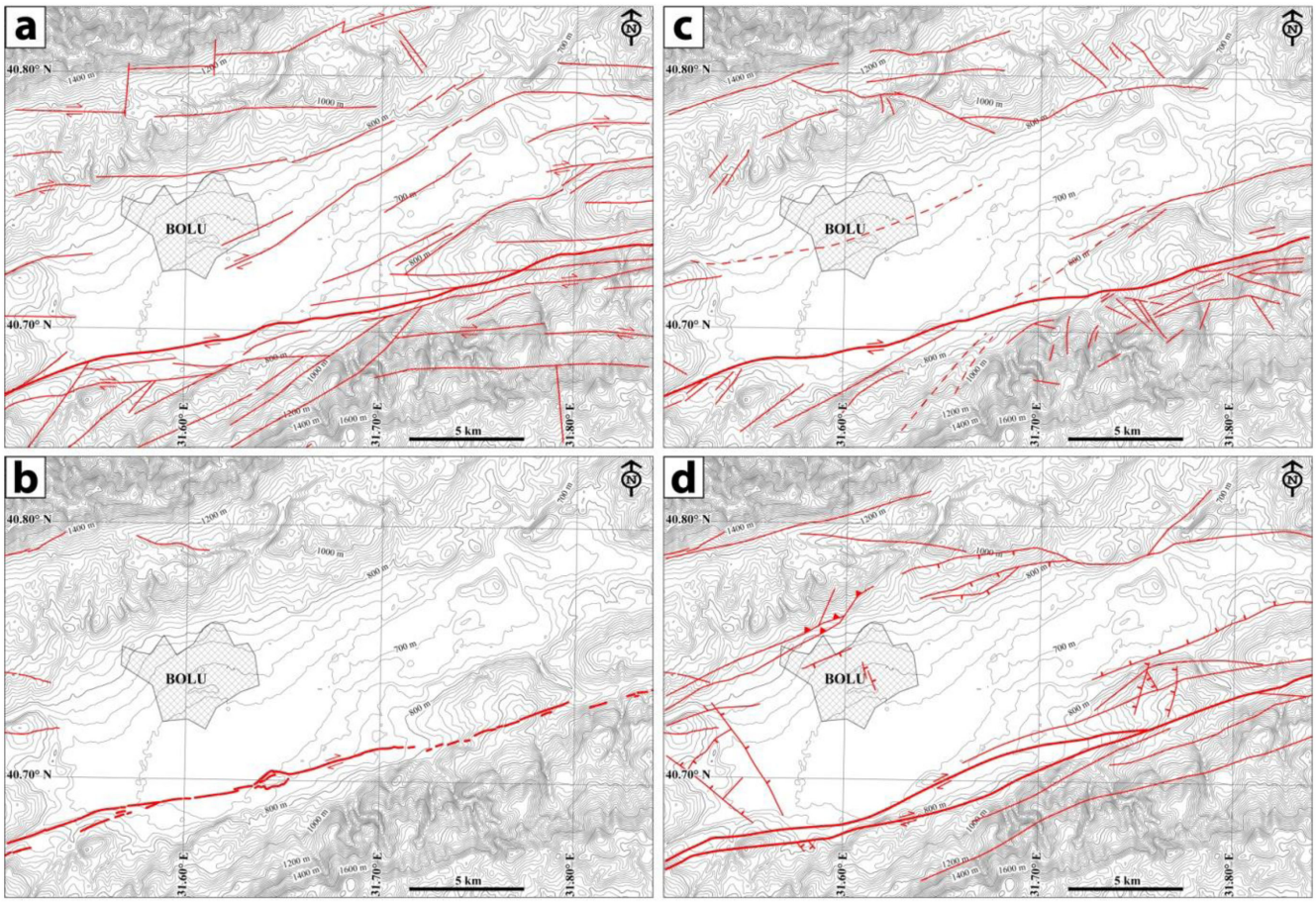


Figure 4. The fault maps from previous morphology-oriented geological studies conducted around Bolu plain. Contours are generated from SRTM elevation data. (a) The faults from Öztürk *et al.* (1985). (b) Active fault map from Emre *et al.* (2011). (c) The faults identified by Aktimur *et al.* (1986). (d) The faults identified by Gökten *et al.* (2011). Please note that most of the fault lines are subparallel to the 1944 Gerede earthquake surface rupture, drawn in the southern part of the Bolu plain.

They concluded that the Düzce Fault and the main strand of the NAFZ are structurally and kinematically linked by the Bakacak and Elmalık faults which are located on a 10–15 km wide right stepover (Fig. 2). No continuation of the Bakacak and Elmalık faults has been reported in the Bolu plain (Hitchcock *et al.* 2003; Başokur *et al.* 2004), but Gökten *et al.* (2011) mentioned the possibility of a prolongation of the active faults, using the evidence of a pressure ridge in the Bolu city centre.

2.2. Field observations

In the SE part of the Bolu plain, we observed a well-developed 75 m wide cataclastic zone in the WNW and ESE of Bürnük village (Fig. 5). At this locality, the cataclastic zone is morphologically marked by gradients and trenches formed by subvertical to steeply dipping fractures (Figs 6a and b).The protolith of the zone is limestone of the Jurassic-Early Cretaceous age. Beds of limestone display NW- and NE-striking, and there is an increase in dip within the zone between 50° and 78°. The cataclastic zone has a high density of brittle deformation features characterized by variably fracturing, lens-shaped structural domains and fault rocks. The zone has variable fracture geometries along the strike, resulting in complex patterns of deformation and fault interaction. Most of fractures are characterized by opening joints that do not show slip surfaces, yet the subvertical NNW-striking joints have irregular surfaces and are generally hydrothermally altered. Limited NNW- and WNW-striking fractures are interpreted to form a conjugate pair that occurs as shear fractures. Locally, anastomosing fractures give rise to lens-shaped blocks in the cataclastic zone, including limestone showing only fractures, suggesting strain partition during formation of the cataclastic zone. Two slickenside surfaces with slickenlines, and four fault surfaces have been measured (Fig. 6c).

Fault plane orientations in the zone are slightly variable, but generally strike N65°–80°W or N80°–85°E and dip 55° to subvertical. Some planes include slickenlines that rake 15°–30° (Fig. 6c). Their sense of slip is not clear, but the pseudo-focal mechanism analysis shows a possible nodal plane with a steeply dipping, approximately east–west striking, right-lateral strike-slip fault (Fig. 6c). Two type fault rocks are exposed around the main fault in the cataclastic zone. These are cohesive fault breccias and cataclasites, which are exposed in the structural domains. Most of the fault breccias have developed on both sides of the main fault (Figs 6a and b) and have a thickness of approximately 1.5 m. The fault breccias consist of angular to subangular clast and lesser amounts of matrix material, which suggest that the limestone was not severely disturbed, but they do show some displacement of fragments. Cataclasites are

Downloaded from https://academic.oup.com/gji/article/201/3/1814/754781 by ANKARA user on 12 December 2021

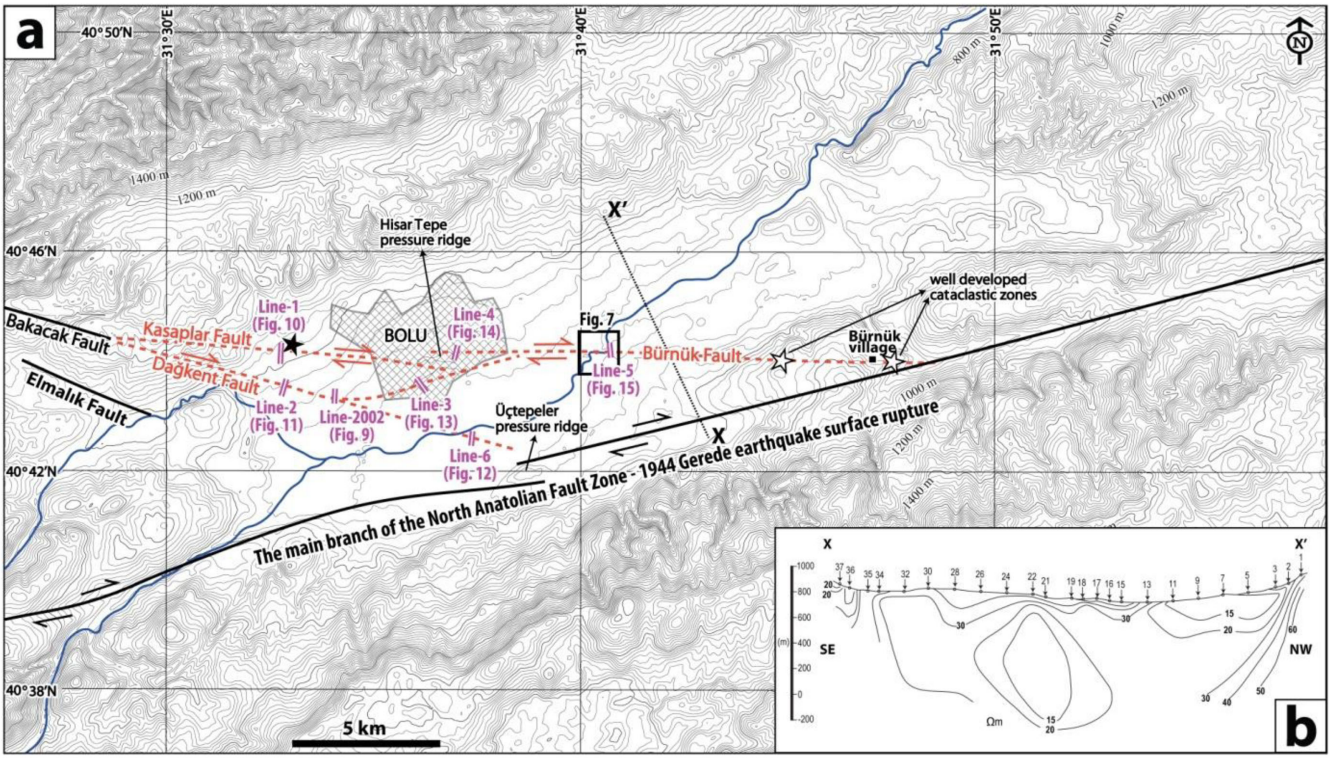


Figure 5. (a) Hypothesized locations of active faults in the Bolu plain based on field observations and geophysical subsurface data. Contours are generated from SRTM elevation data. White stars indicate the locations of well-developed cataclastic zones. Black star shows the location of fault surfaces with hydrothermal activity. The black square shows the diversion of the Büyüksu River. Line-2002 is the previous seismic reflection line. The six seismic reflection lines were planned to check this hypothesis (b) Iso-resistivity cross section X–X' from Herece (2005) having an anomaly corresponding to the Bürnük Fault.

seen locally and are well developed when very close to the fault surface. They are matrix-supported, indicating that shear displacement here is much larger than that of the breccia. The cataclasites have a thickness of up to 0.2 m.

All these structures within the cataclastic zone described above are attributed to the WNW–ESE trending Bürnük Fault. The WNW continuation of the Bürnük Fault in the Bolu plain corresponds to the 550 m right-lateral diversion of the Büyüksu River (Fig. 7).

In the NW part of Bolu plain, a few fault surfaces (N65W, 80NE) showing traces of hydrothermal activity with no slickenlines are observed, and they provide a clue to the location of the Kasaplar Fault (Fig. 5).

On the asphalt road in Bolu city centre, a persistent crack that reappears after every repair attempt has been reported by local people. We examined this feature and evaluated it as a sigmoidal opening fracture (Fig. 8) that indicates a NE–SW trending right-lateral shear. The constant reappearance of this fracture may indicate creep on the fault zone, and therefore this location was deemed worth examining by seismic reflection study.

2.3 Available geophysical subsurface data

Herece (2005) reported an iso-resistivity section in the Bolu plain (Fig. 5b). The data show a resistivity anomaly which was interpreted as a sign of a north dipping normal fault by Herece (2005), and that is also seen in the map of Gökten *et al.* (2011; Fig. 4d). We suggest that this anomaly corresponds to a continuation of the Bürnük Fault in the Bolu plain (Fig. 5).

The possibility of a continuation of the Düzce/Bakacak Fault into the Bolu plain has been investigated west of Bolu but insufficient evidence was found (Başokur *et al.* 2004). On the other hand, a single seismic study performed during 2002 indicated a fault zone under the Bolu plain (Gündoğdu 2010). The reinterpreted seismic section of Line-2002 (Fig. 9) demonstrates that there is a fault located at 190 m and extending as a vertical line dividing the two compartments of different seismic characteristics. There are two, less distinctive fault lines on both sides, that can be recognized by the discontinuity of the seismic layers. The clearly observed fault on Line-2002 indicates that the continuation of Bakacak fault exists under the Bolu plain (Figs 5 and 9).

2.4 The hypothesis of active faulting in the Bolu plain

Bringing the previously obtained information together with our field observations and available subsurface data allows us to hypothesize that the connection between the Düzce/Bakacak faults and the main strand of the NAFZ lies on the eastern tip of the Almacık block (Fig. 5). We speculate that the eastern continuation of the Bakacak Fault (Hitchcock *et al.* 2003) has two branches. The northern branch is composed of the Kasaplar and Bürnük faults and the Hisar Tepe pressure ridge is located in the restraining offset among them. The Bürnük Fault has a well-developed cataclastic zone and has created a diversion on the Büyüksu river and a resistivity anomaly (Fig. 5). The southern branch, the Dağkent Fault, might provide a link between the Bakacak Fault and the fault observed in the 2002 seismic reflection line. There are two possibilities for the SE continuation of the Dağkent Fault. The first is a linear route towards the main branch of the NAFZ that is along the 1944 Gerede earthquake surface rupture. The second is a bend towards the NE via the shear zone observed in Bolu city centre. In order

Downloaded from https://academic.oup.com/gji/article/201/3/1814/754781 by ANKARA user on 12 December 2021

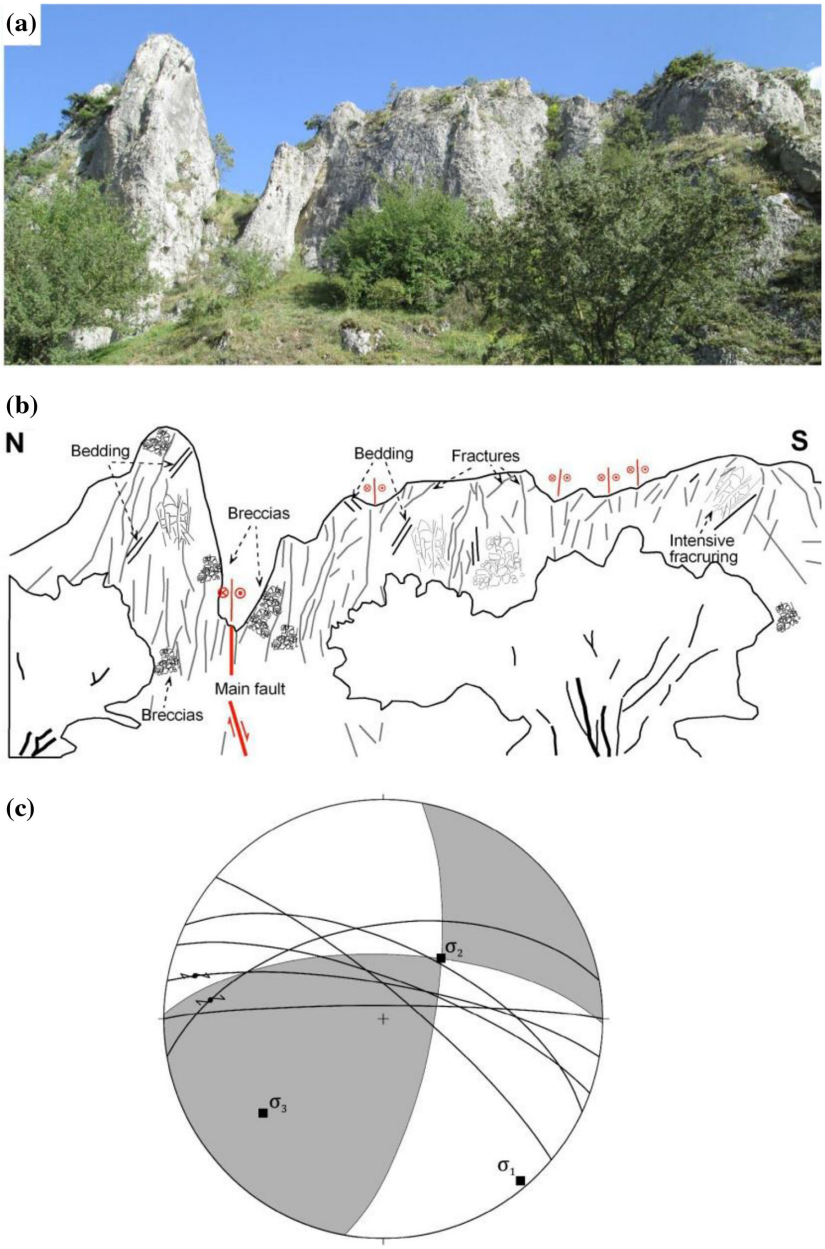


Figure 6. (a) Field photograph of the cataclastic zone on the Bürnük Fault. For location see Fig. 5. (b) Line drawing of the outcrop in (a) that shows internal structures of the cataclastic zone. Note the abundance of fractures and the formation of fault rocks. (c) Equal-area lower hemisphere projection of fault planes measured on the main fault. The $\sigma 1$, $\sigma 2$ and $\sigma 3$ indicate the maximum, intermediate and minimum principal stress axes, respectively.

to test the hypothesis about the active faulting in the Bolu plain, six seismic reflection lines were planned, the results of which will be discussed with the seismological data in the following sections (Fig. 5).

3 METHODS OF SEISMIC REFLECTION STUDIES AND SEISMOLOGY

3.1 Seismic reflection data acquisition, data quality control and data processing

A P-Gun (Buffalo-Gun) of 36 barrels with 50 gr. pellets was used as a Seismic Energy Source. Line-5 and Line-6 were shot using the P-Gun. The P-Gun generates a 94 ton pick-force, and provides more than 1000 m in penetration depth. The upper frequency limits of the P-Gun generated seismic signals were 100–120 Hz. In the city centre, Line-3 and Line-4 were shot by a weight-drop type of seismic energy source, mounted on a small-vehicle. A 300 kg steel-cylinder was dropped from a height of 1.5 m, and a penetration depth of 500 m was achieved. Seismic signals generated by weight-drop may reach up to 90–100 Hz frequencies.

96 vertical geophones of 14 Hz each were used as seismic receivers. One geophone per receiver station was planted. 4 Geometrics Geode modules, each controlling 24 channels, were used as part of the seismic recorder system. The time-break was achieved by a shot-geophone attached to the P-Gun's body.

Downloaded from https://academic.oup.com/gji/article/201/3/1814/754781 by ANKARA user on 12 December 2021

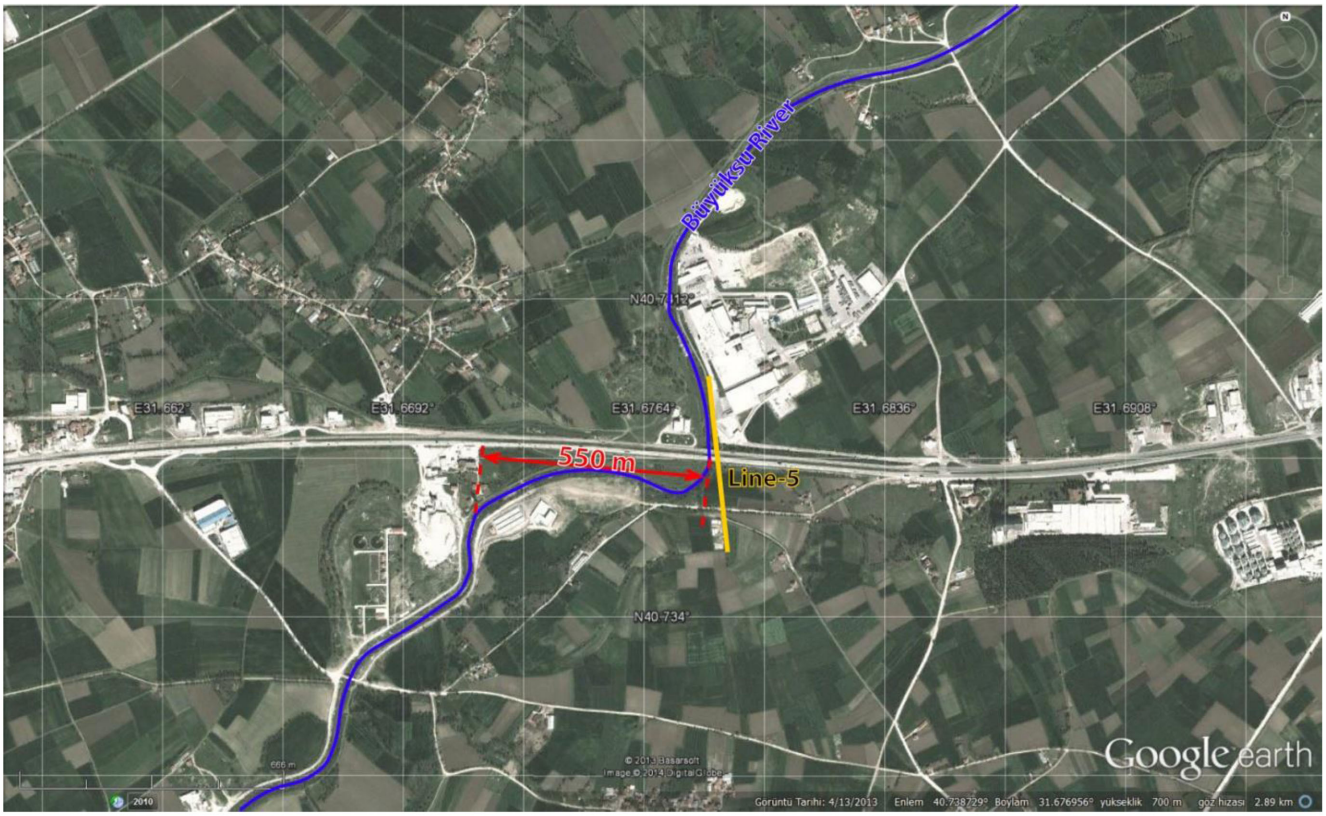


Figure 7. Diversion of the Büyüksu River along the Bürnük Fault. For location see Fig. 5.

Sampling intervals of 1 ms, and recording times of 4 s were chosen for the P-Gun surveys. Sampling intervals of 0.5 ms, and recording times of 2 s were chosen for the Weight-drop surveys. One vertical-stack was sufficient for signal enhancement. No analogue or digital filters were used during the data acquisition.

A walk-away type of field-spread was used. In the case of the P-Gun, the receiver interval was 5 m, the shot interval was 5 m and the spread-length was 475 m. In the case of the weight-drop, the receiver interval was 2 m, the shot interval was 4 m and the spread-length was 190 m. The vertical resolution was given as one quarter of the dominant wavelength, in accordance with Widess (1973). If we assume an average velocity of 1800 m s^{-1} in alluvium, and a dominant frequency 30 Hz of the seismic wavelet, the resolution may be computed as 15 m.

To ensure a good signal-to-noise ratio, shot stations were selected at those road-sites where traffic noise was low. When seismic lines were spread along a road-side, police or gendarme forces were called to temporarily halt the traffic.

The Data-Processing sequences are: Geometry definition, Bandpass filter, Automated-gain-control, Trace-edit, First-break mute, Ground-roll mute, Data-resample, Common-depth-point sort, Velocity-Analysis with Interactive Constant-velocity-scan, Stack, Trace-mix and Time-to-depth conversion.

When needed, a second Bandpass filter and a second Automated-gain-control were added to the Job-stream. A Notch-filter was applied when a seismic-line passed through city power-lines. Since the terrain was almost flat, no static corrections were applied to the data for Line-3, Line-4 and Line-6. Static correction was applied to Line-5. We did not apply a Migration process to the data due to the shortness of the seismic sections (the stacked-data comprised around 100 traces).

3.2 Seismological processes

In the seismological processes, before computing focal mechanism solutions, a relocation procedure was applied to the events recorded by the Kandilli Observatory and Earthquake Research Institute (KOERI) in order to minimize the location errors in both vertical and horizontal directions and to determine robust hypocentre parameters. We repicked all *P* and *S* phases arrival times and then relocated the events by using the Hypoinverse-2000 earthquake location software (Klein 2002). During the relocation process, a 1-D *P*-wave crustal velocity model given in Bekler & Gürbüz (2008) was used. In this procedure we also recomputed the local magnitudes of the events.

One of the goals of this paper was to obtain focal mechanism solutions for some of the earthquakes that have occurred in the region. Thus we performed the time domain regional moment tensor inversion following Herrmann *et al.* (2011) in order to determine the source depth, moment magnitude and strike, dip and rake angles of a shear-dislocation source by using three-component broadband waveforms. The main purpose of this method is to fit synthetic waveforms to observed seismograms at local and regional stations. The synthetic Green's functions were computed as suggested in Herrmann *et al.* (2011). Both the observed and Green's function ground velocities were cut from 10 s before the *P*-wave's first-arrival to about 180 s after it. In the inversion process a three-pole causal Butterworth bandpass filter changing with a 0.06–0.14 Hz band range was used for the events. Additionally, when needed an optional microseism rejection filter was applied to enhance the signal-to-noise ratio. We eliminated noisy and problematic signals; furthermore, waveform data recorded by stations beyond 700 km were deselected.

Downloaded from https://academic.oup.com/gji/article/201/3/1814/754781 by ANKARA user on 12 December 2021

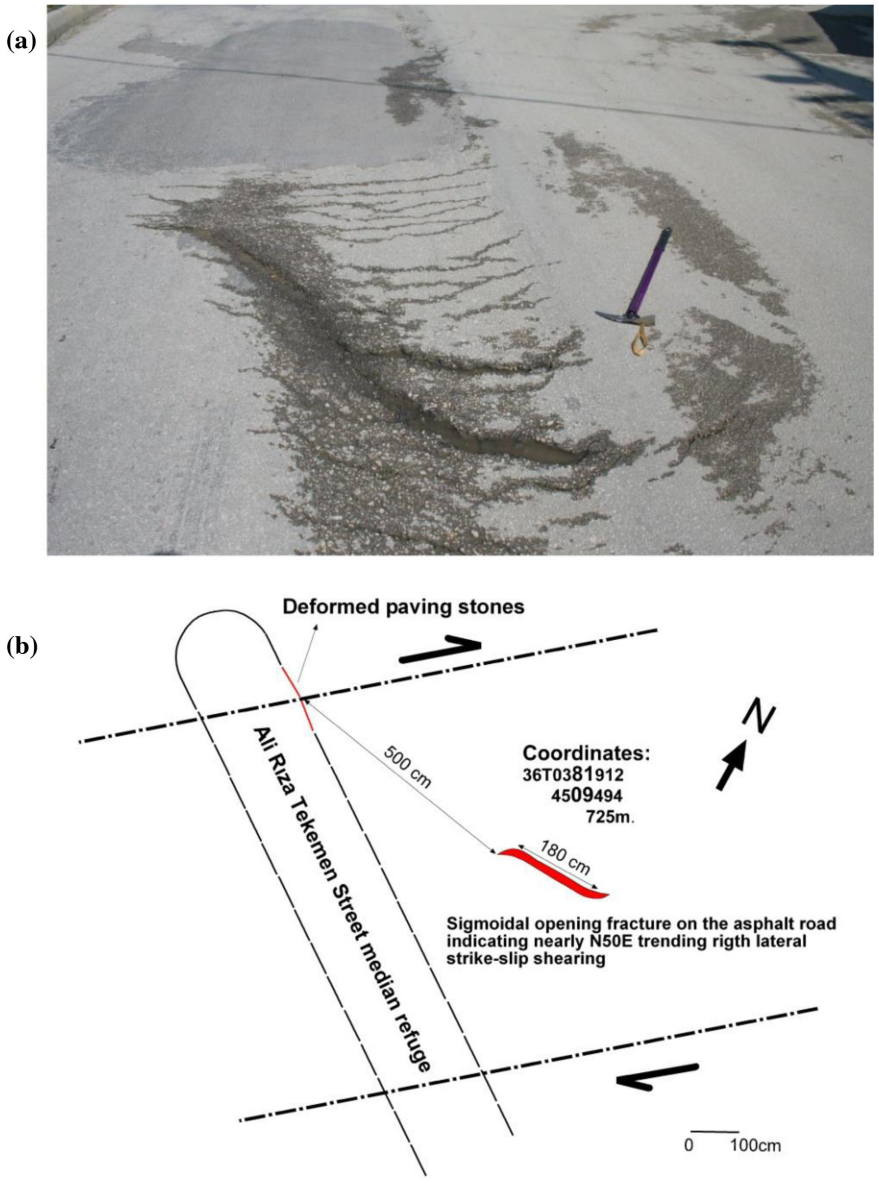


Figure 8. (a) A photograph of the sigmoidal opening fracture in the Bolu city centre. (b) A sketch of the structure.

4 ACTIVE FAULTING IN THE BOLU PLAIN BASED ON SEISMIC REFLECTION STUDIES AND SEISMOLOGY

4.1 Interpretation of seismic reflection lines

Line-1 was planned to test the existence of the Kasaplar Fault, the northern branch of the Bakacak Fault under Bolu plain (Figs 5 and 10). In the seismic reflection section of Line-1, the main shearing on the Kasaplar Fault is seen between 200 and 230 m as indicated by weak-continuation or discontinuity of the reflections. The overall shape of the Kasaplar Fault and its branches resembles a positive flower structure. The transpressional character of the Kasaplar Fault can be determined by the anticline shape of the seismic layers and especially the dominant reverse faulting component seen among the seismic layers at the upper right-hand side of the seismic section (Fig. 10).

The southern continuation of the Bakacak Fault under the Bolu plain, the Dağkent Fault, was recognized by a seismic study performed during 2002 (Gündoğdu 2010; see Fig. 9 for a reinterpretation). Line-2 is planned to consolidate the position of the Dağkent Fault. The seismic section of Line-2 clearly demonstrates a vertical main fault at 36 m that is recognized by the sudden discontinuity of a seismic layer at the top of the southern block (Fig. 11). On the northern block, a less distinctive branch of the Dağkent Fault is also seen (Fig. 11). The strike obtained from Line-2002 and Line-2 for the Dağkent Fault leads us to check its continuation towards the SE. For this reason, Line-6 was investigated, but it showed no sign of fault trace (Fig. 12). Therefore the other possibility for the continuation of Dağkent Fault was taken into account. Line-3 is oriented normal to the shear zone as determined by the sigmoidal opening fracture in the Bolu city centre. The main fault is located between 85 and 107 m and its several branches merge at a depth of 500 m (Fig. 13). There is a small asymmetrical sedimentary depression

Downloaded from https://academic.oup.com/gji/article/201/3/1814/754781 by ANKARA user on 12 December 2021

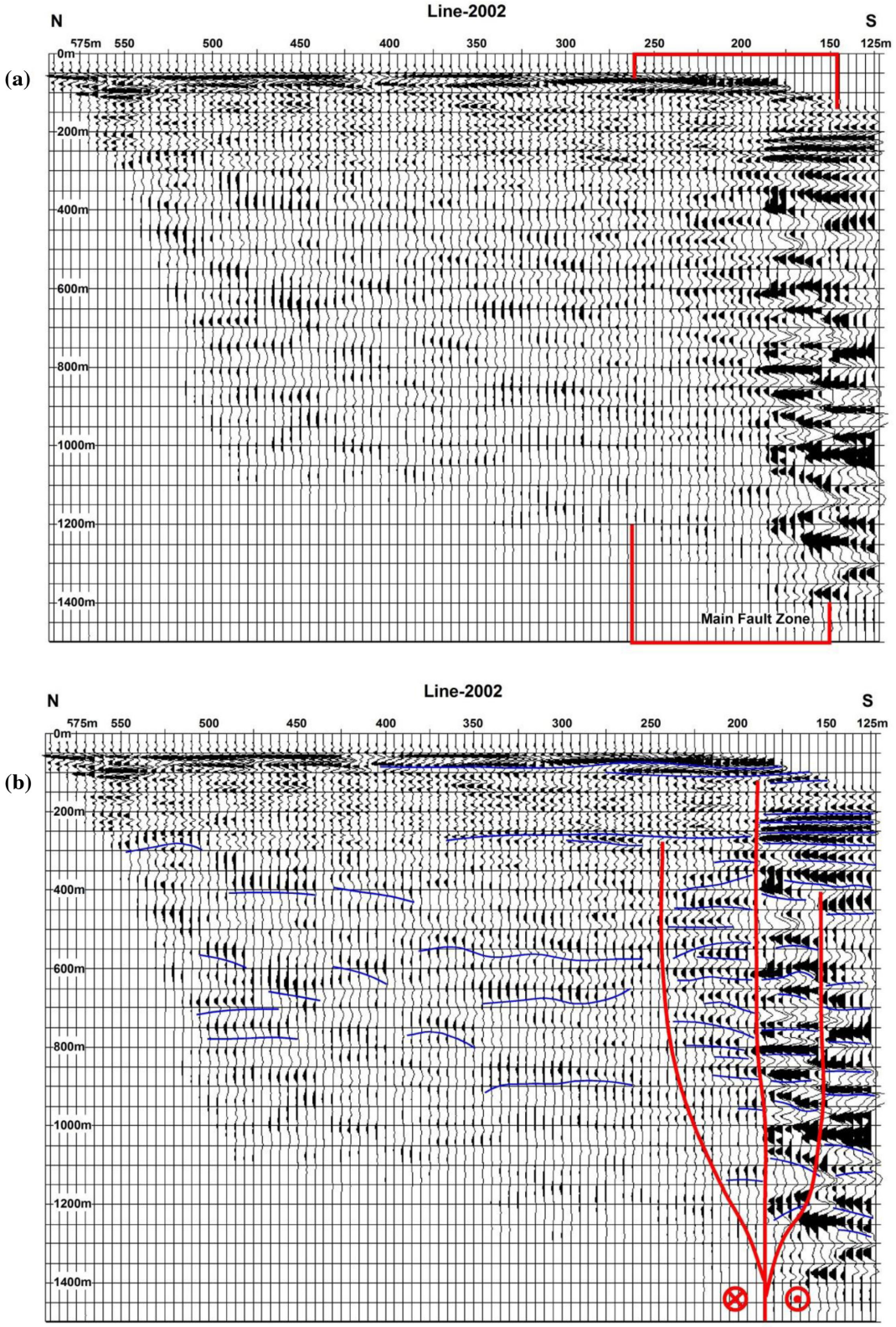


Figure 9. Seismic reflection of Line-2002. (a) Uninterpreted and (b) interpreted. For location see Fig. 5.

filled by nearly horizontal layers that can be distinguished at the top of the seismic section. Determination of the faulting on the seismic section of Line-3 gives rise to the possibility that the NW–SE trending Dağkent Fault detected in seismic sections at Line-2002 and Line-2 bends towards the NE after being invisible on Line-6 (Fig. 12).

We postulated that the Hisar Tepe pressure ridge is located on the restraining stepover between the Kasaplar Fault and the Bürnük

Downloaded from https://academic.oup.com/gji/article/201/3/1814/754781 by ANKARA user on 12 December 2021

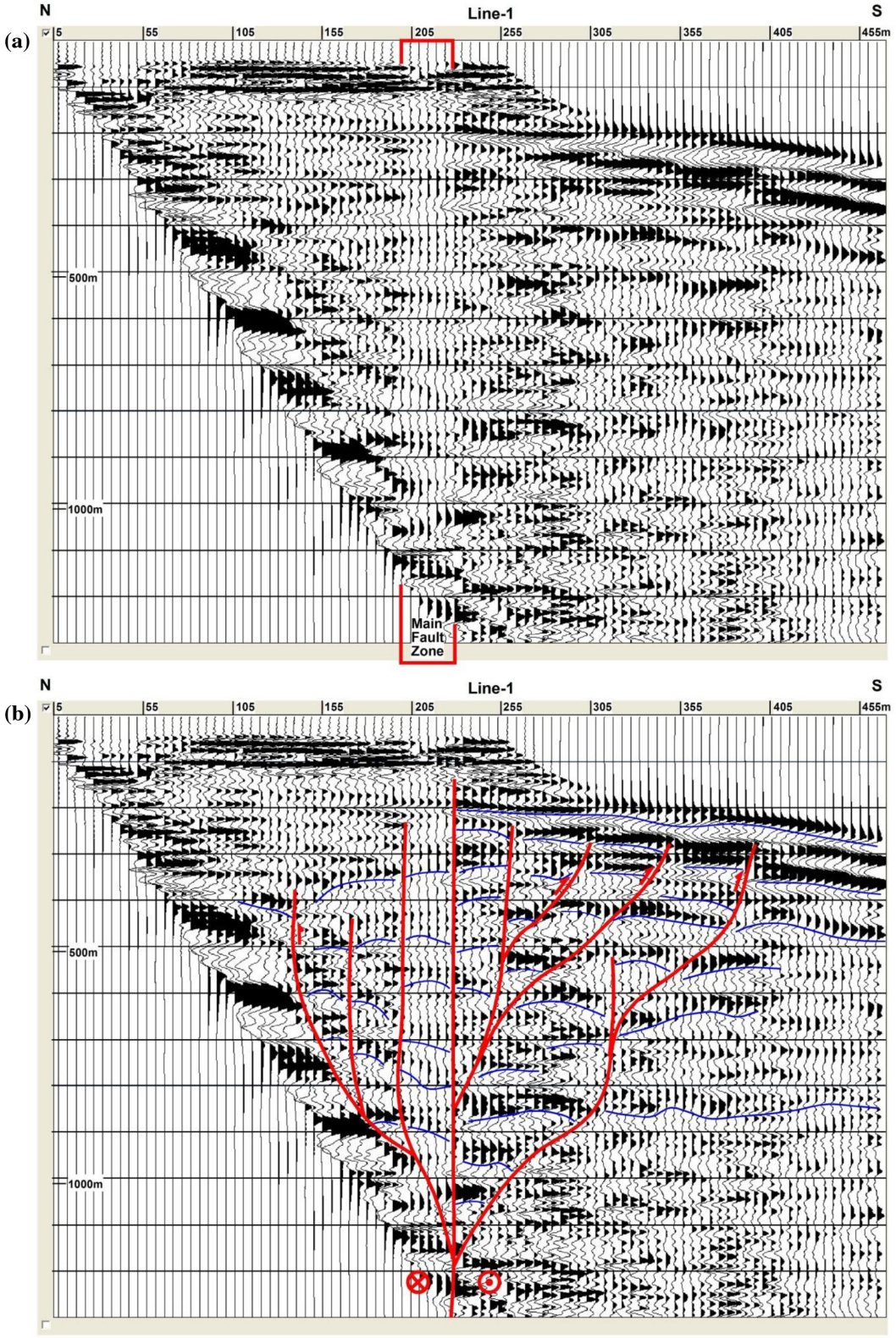


Figure 10. Seismic reflection of Line-1. (a) Uninterpreted and (b) interpreted. For location see Fig. 5.

Fault. The western end of the Bürnük Fault should be located to the north of Hisar Tepe to create this pressure ridge. Line-4 was designated to test this location (Figs 5 and 14). In the seismic section of Line-4, a fault zone is seen between 92 and 105 m. The faults can be extended to the surface down to a depth of 75 m (Fig. 14).

Line-5 is located near a sharp bend on the Büyüksu River (Fig. 5). The seismic section of Line-5 has a zone of weak reflections between

Downloaded from https://academic.oup.com/gji/article/201/3/1814/754781 by ANKARA user on 12 December 2021

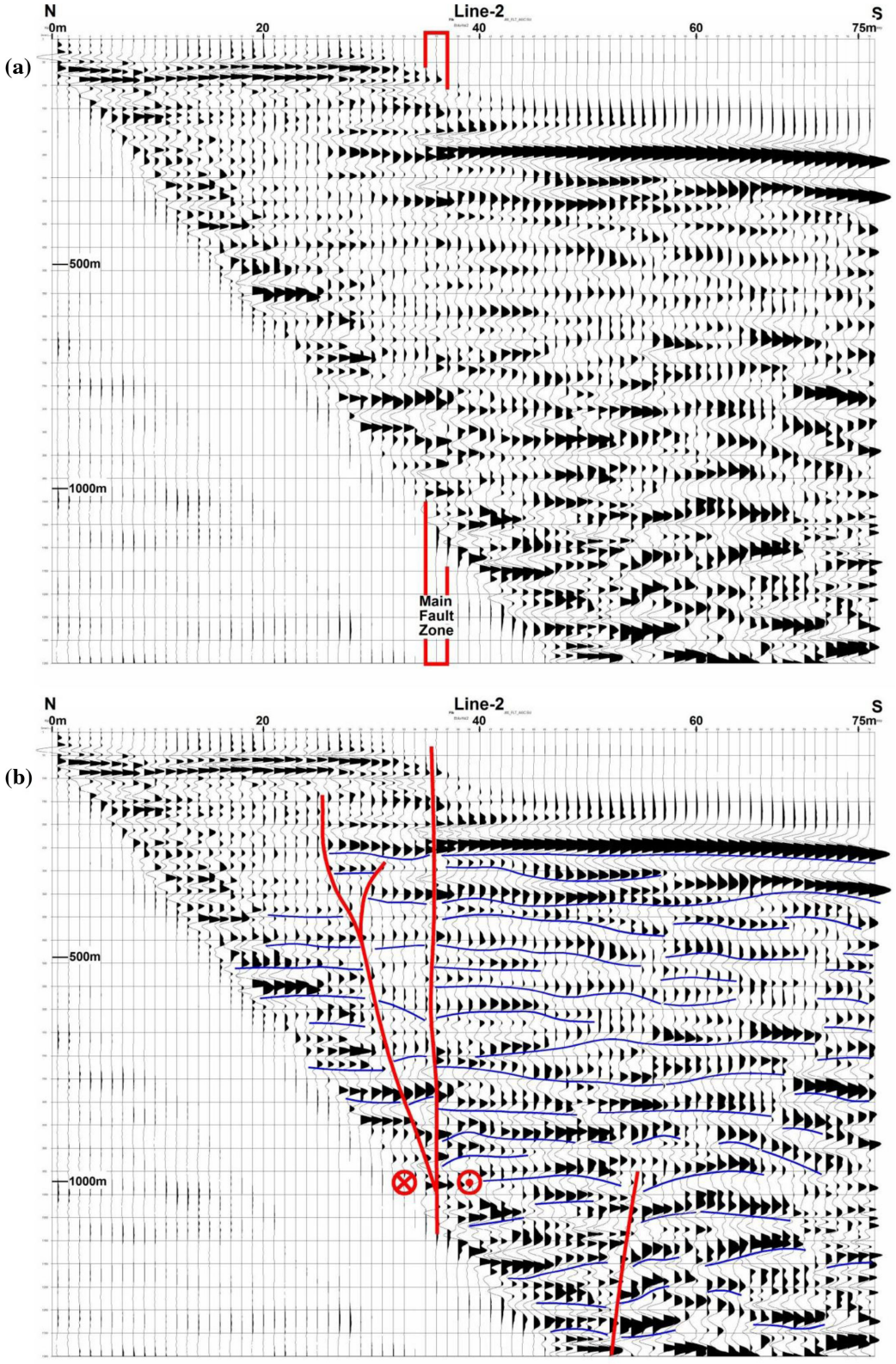


Figure 11. Seismic reflection of Line-2. (a) Uninterpreted and (b) interpreted. For location see Fig. 5.

Downloaded from https://academic.oup.com/gji/article/201/3/1814/754781 by ANKARA user on 12 December 2021

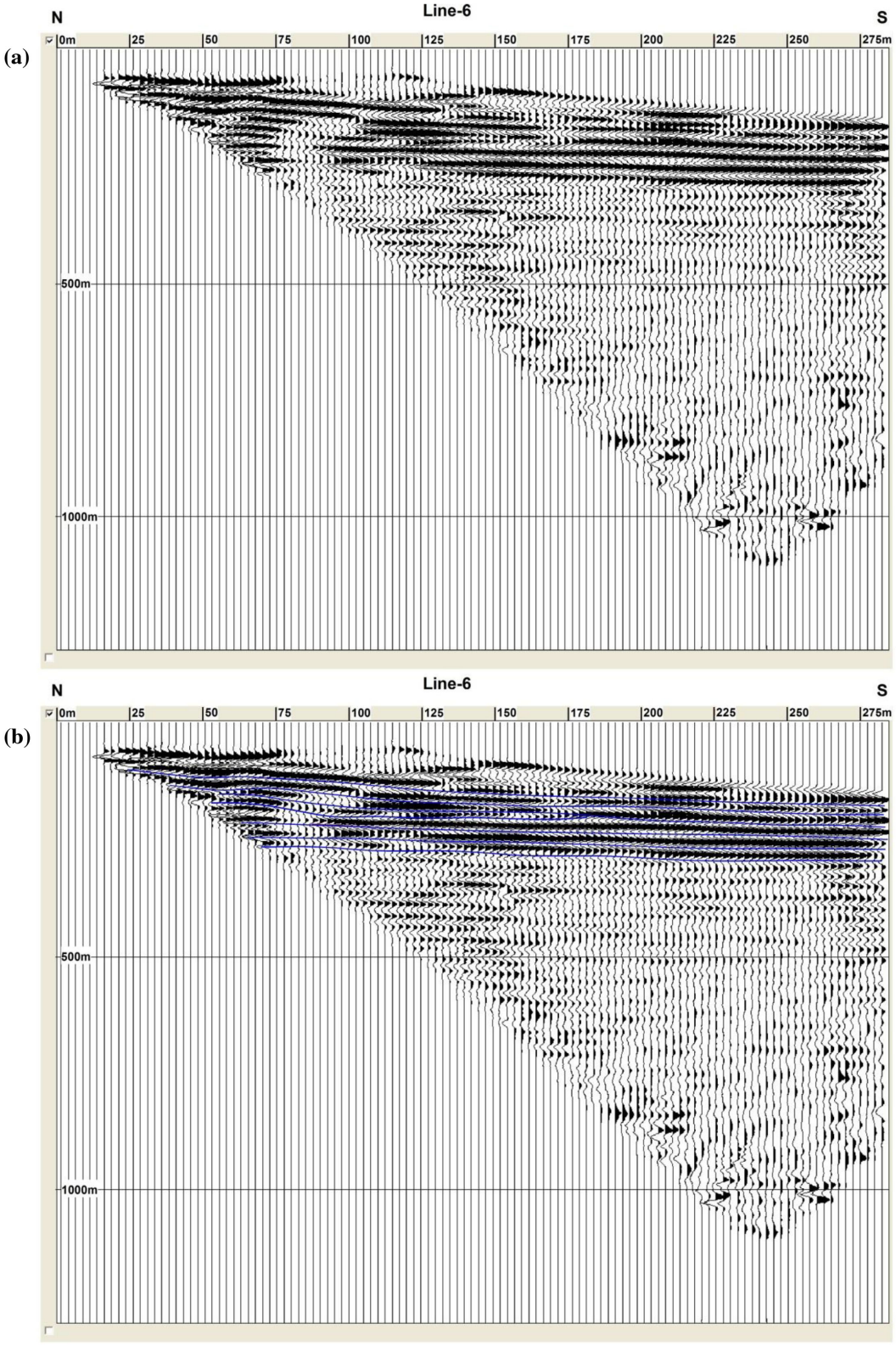


Figure 12. Seismic reflection of Line-6. (a) Uninterpreted and (b) interpreted. For location see Fig. 5.

Downloaded from https://academic.oup.com/gji/article/201/3/1814/754781 by ANKARA user on 12 December 2021

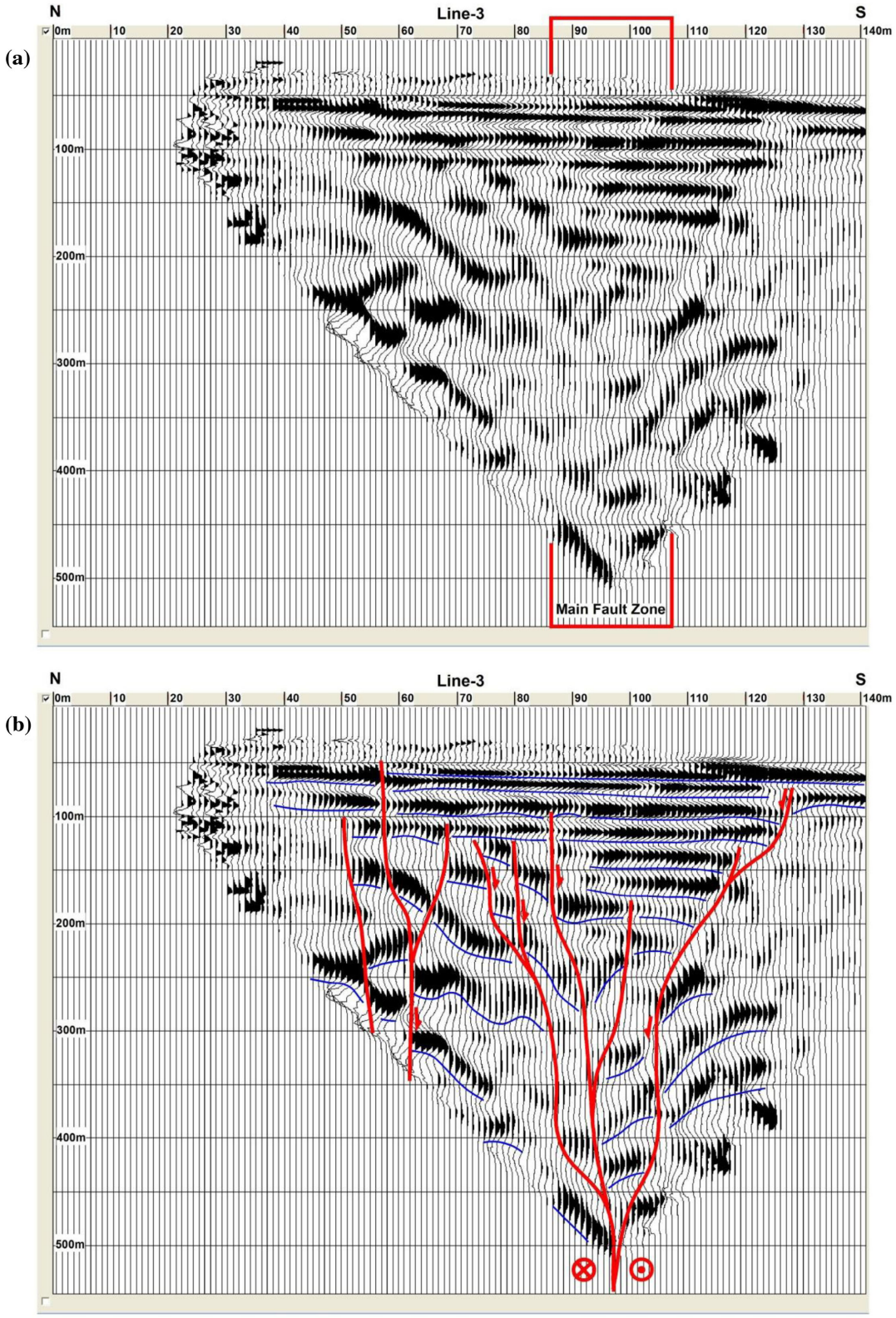


Figure 13. Seismic reflection of Line-3. (a) Uninterpreted and (b) interpreted. For location see Fig. 5.

Downloaded from https://academic.oup.com/gji/article/201/3/1814/754781 by ANKARA user on 12 December 2021

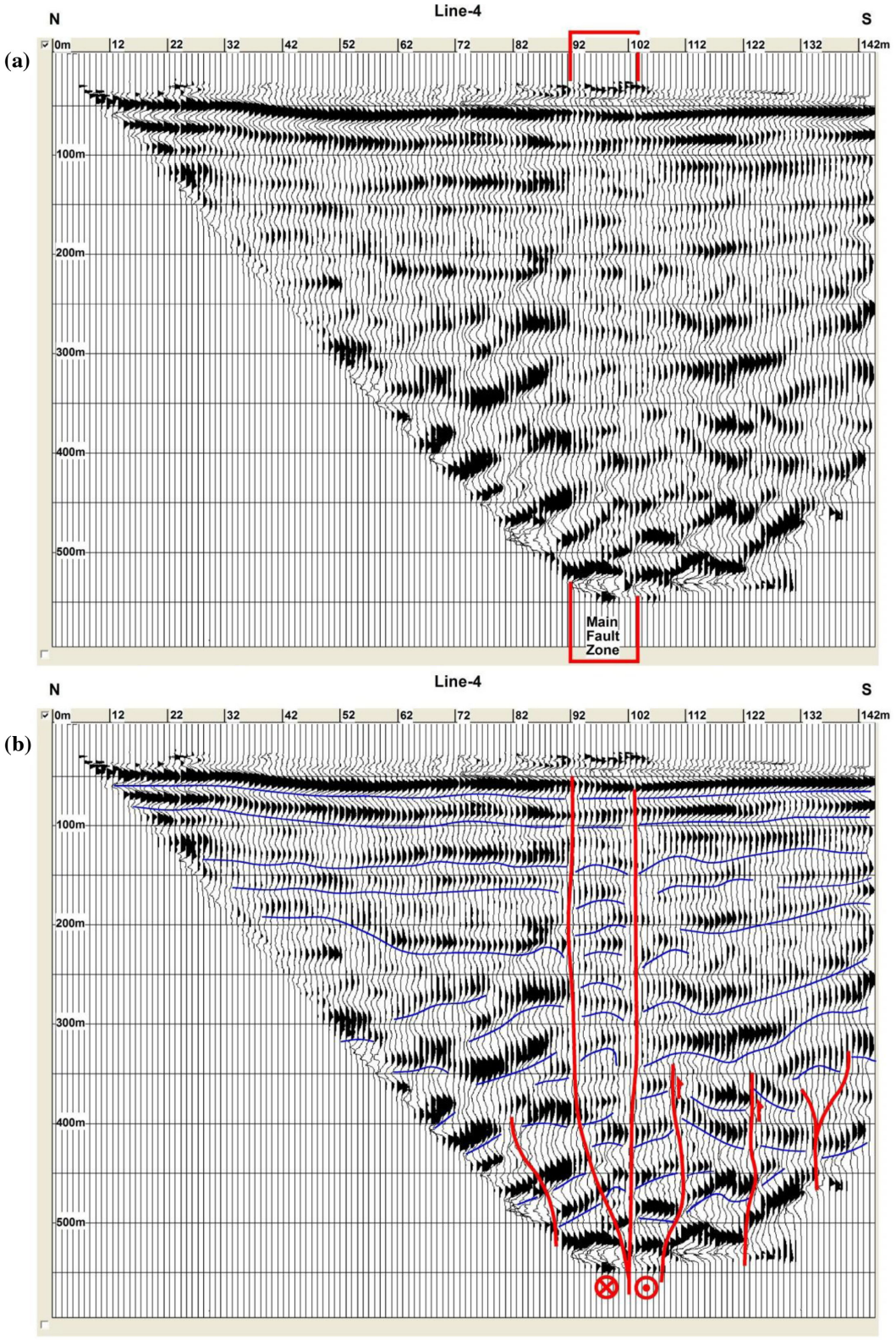


Figure 14. Seismic reflection of Line-4. (a) Uninterpreted and (b) interpreted. For location see Fig. 5.

Downloaded from https://academic.oup.com/gji/article/201/3/1814/754781 by ANKARA user on 12 December 2021

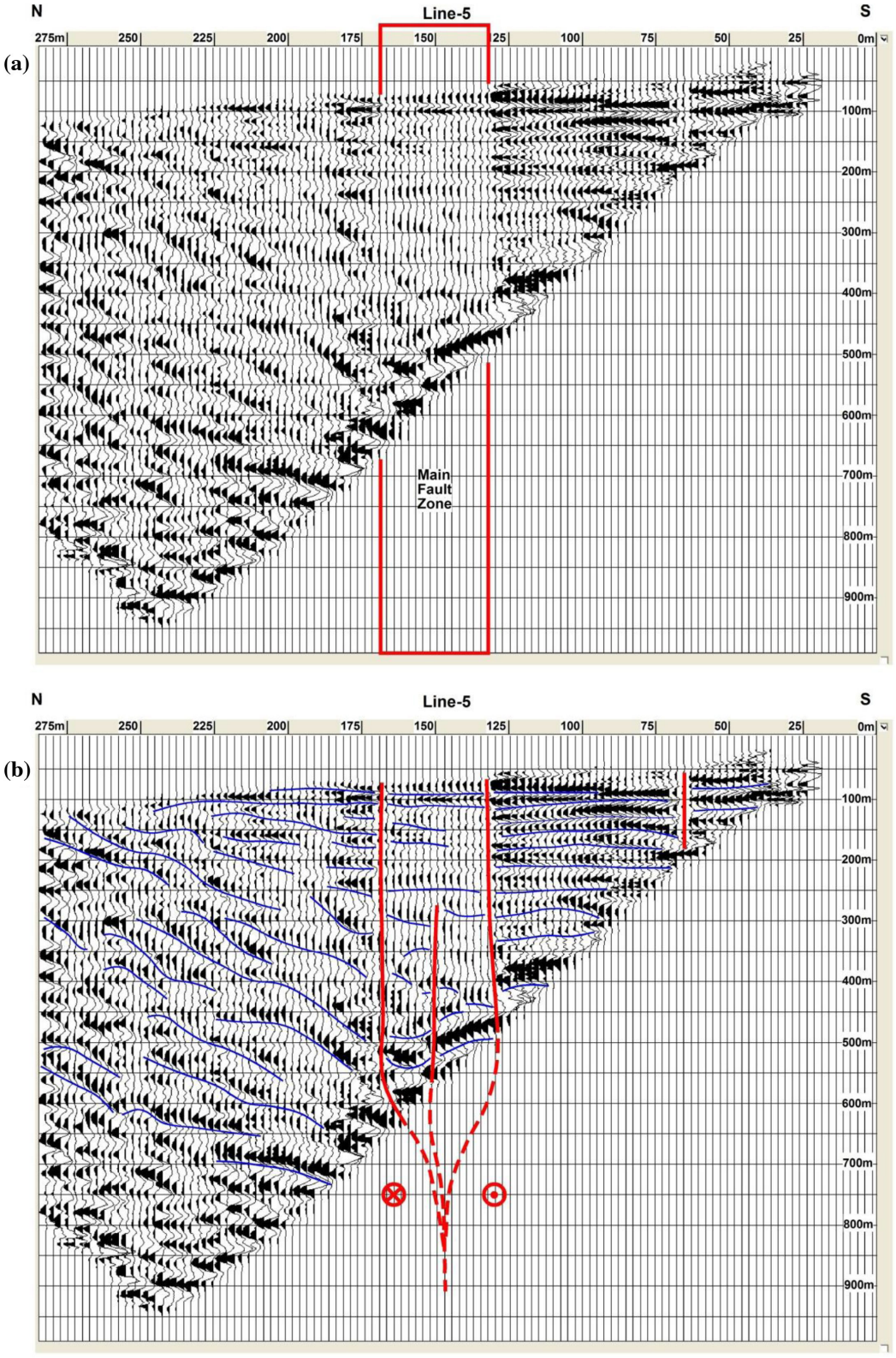


Figure 15. Seismic reflection of Line-5. (a) Uninterpreted and (b) interpreted. For location see Fig. 5.

Downloaded from https://academic.oup.com/gji/article/201/3/1814/754781 by ANKARA user on 12 December 2021

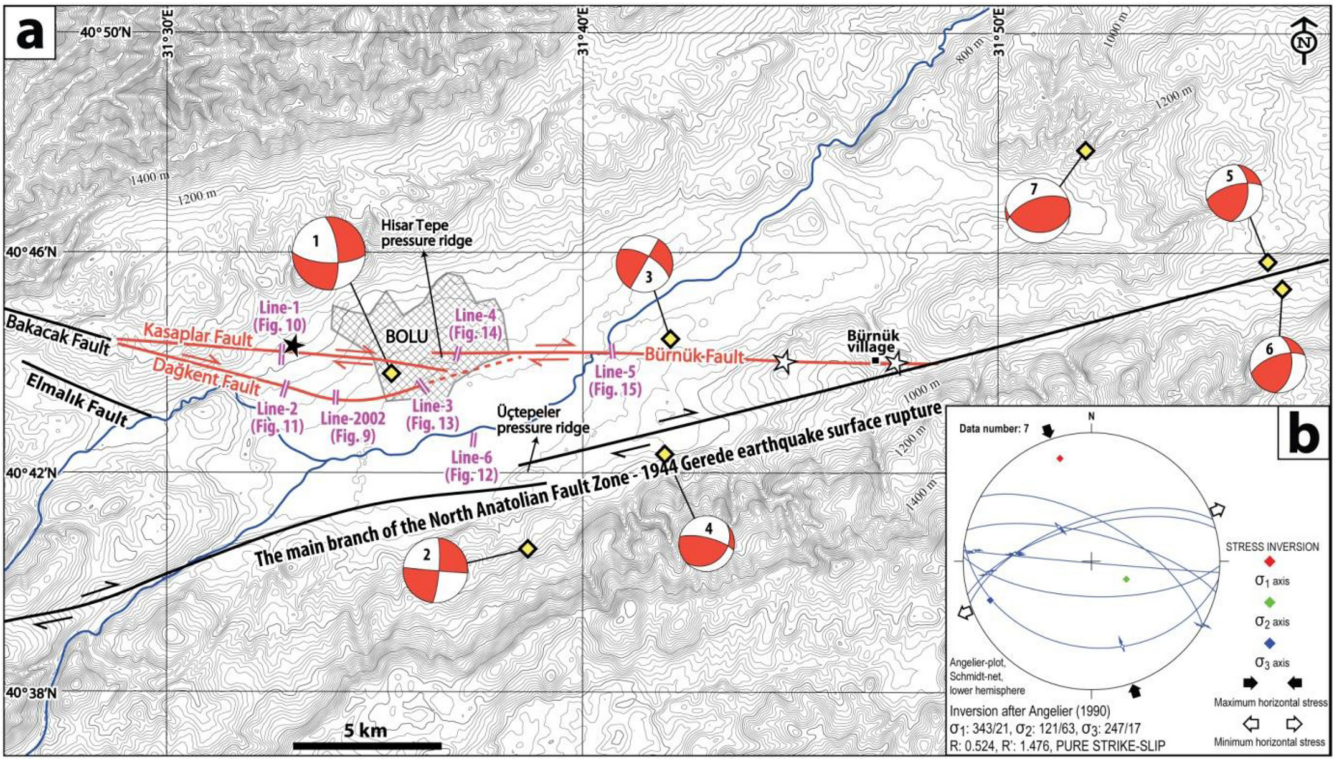


Figure 16. (a) Active faults in the Bolu plain tested by seismic reflection studies. See Table 1 for the details of focal mechanism solutions. (b) Stress analysis from the focal mechanism solutions indicates a pure strike-slip regime rather than the previously suggested transtension. SG2PS software (Sasvári & Baharev 2014) with Angelier's (1990) inversion method was used for the stress analysis.

133 and 158 m that would correspond to the Bürnük Fault (Fig. 15). The evidence from Line-4, Line-5 and cataclastic zone observations around Bürnük village indicates that the Bürnük Fault is located between Hisar Tepe and the east of Bürnük village. The Kasaplar and Bürnük faults in the Bolu plain are the missing link between the Bakacak Fault and the main branch of the NAFZ that was proven by the 1944 Gerede earthquake's surface rupture (Fig. 16).

4.2 Focal mechanism solutions of recent earthquakes

The seven significant earthquakes that occurred just beneath the city centre of Bolu and to its east, after the main shock of the 1999 November 12 Düzce earthquake, were selected in order to determine their source parameters (Fig. 16). Before the process of focal mechanism solutions, all events except the first one were relocated. The computed relocation parameters are given in Table 1. After the relocation process, root mean square (rms) times and location errors were reduced significantly.

The first two events, the 1999 November 16, 17:51:18 (UTC) earthquake (M_w = 5.3) and the 2004 April 13, 21:47:24 (UTC) earthquake (M_L = 4.3), could not be analyzed for source parameter inversion because of a lack of digital waveform data. Hence their focal mechanism solutions were obtained from the Swiss Seismological Service (SSS) at the ETH Zurich catalogues.

Two earthquakes on 2005 July 10 occurred successively around the city centre of Bolu at 07:08:27 and 07:28:43 (UTC) with a magnitude of 3.5 and 3.4, respectively. The other two events occurred sequentially on 2008 November 12 at 11:57:34 (UTC) (M_L = 4.1) and at 14:25:43 (UTC) (M_L = 3.9). The last event was on 2013 November 24 at 20:49:38 (UTC) (M_L = 5.0), respectively. The most recent three earthquakes were located further east than the previous four events.

As an example of the processing, we give here the most recent event (M_L = 5.0) of 2013 November 24, 20:49:38 (UTC). A total of 36 stations were selected in the regional moment tensor inversion for this event. The selected stations are shown in Fig. 17. After the inversion processes, a correlation of the reduction in distance-weighted variance against to source depth was plotted (Fig. 18). The best fit was obtained at a depth of 8 km, by plotting the best mechanisms associated with each source depth. The comparisons of the observed and predicted waveforms are shown in Fig. 19. In almost all waveforms there is a fit between the observed and predicted waveforms.

The source parameters of the five significant earthquakes are given in Table 1. On the basis of the computation solutions, the source parameters of the events (1 and 3) show an agreement with the faults determined in this paper.

5 DISCUSSIONS

The seismic reflection studies determined the Kasaplar, Dağkent and Bürnük faults in the Bolu plain. The Hisar Tepe pressure ridge may have developed between the Kasaplar and Bürnük faults. These faults are the missing link between the Bakacak Fault and the main branch of the NAFZ. The recent surface ruptures of the 1944 February 01 Gerede, 1957 May 26 Abant, 1967 July 22 Mudurnu, 1999 August 17 Kocaeli and the 1999 November 12 Düzce earthquakes

Downloaded from https://academic.oup.com/gji/article/201/3/1814/754781 by ANKARA user on 12 December 2021

Table 1. Hypocentral and source parameters of the selected earthquakes in the region.

	Hypocentral parameters									Source parameters								
										Nodal Planes								
													P		T			
Nos.	Date (dd/mm/yyyy)	Time (UTC)	Lat. N(°)	Lon. E(°)	Depth (km)	Mag (s)	rms (km)	ErH (km)	ErZ	M_w	Strike1(°) Strike2(°)	Dip1(°) Dip2(°)	Rake1(°) Rake2(°)	Azimuth (°)	Plunge (°)	Azimuth (°)	Plunge (°)	Reference
1	16/11/1999	17:51:18	40.7300	31.5900	5.0	5.3 (M_w)	–	–	–	5.0	354 92	70 68	−23 −159	312	30	43	1	SSS
2	13/04/2004	21:47:24	40.6777	31.6447	8.7	4.3 (M_L)	0.12	0.55	0.74	4.4	95 5	89 81	−171 −1	320	7	229	6	SSS
3	10/07/2005	07:08:29	40.7395	31.7012	15.6	3.5 (M_L)	0.21	0.99	0.92	3.6	210 300	90 65	−25 −180	162	17	258	17	This study
4	10/07/2005	07:28:43	40.7068	31.6985	15.0	3.4 (M_L)	0.15	0.66	0.81	3.6	284 45	73 30	115 35	354	24	225	55	This study
5	12/11/2008	11:57:34	40.7653	31.9403	10.8	4.1 (M_L)	0.32	0.33	1.42	3.9	255 5	67 50	136 30	314	11	212	46	This study
6	12/11/2008	14:25:43	40.7565	31.9460	11.8	3.9 (M_L)	0.21	0.33	1.44	3.7	251 5	64 50	134 35	311	8	211	50	This study
7	24/11/2013	20:49:38	40.7980	31.8675	15.5	5.0 (M_L)	0.18	0.30	1.33	4.8	250 98	60 33	75 114	351	14	126	71	This study

occurred around the Almacık block, except for the Kasaplar and Bürnük faults in the Bolu plain. These constitute the non-ruptured NE part of the Almacık block and have become the best candidate for a future earthquake source following the 1999 November 12 event.

The existence of the Kasaplar and Bürnük faults has been demonstrated by seismic reflection studies. Their activity is proven by recent earthquakes (events 1 and 3) that have occurred on or near the line of these faults and that clearly provide right-lateral strike-slip focal mechanism solutions. The evaluation of recent seismic activity on the Bolu plain (Fig. 16b) presents a pure strike-slip character which is different from the transtensional nature previously suggested (Özden *et al.* 2008; Gökten *et al.* 2011). This result demonstrates that even if the Quaternary Bolu Basin was developed as a pull-apart structure, the recently established active fault network of the eastern Almacık block has terminated the pull-apart nature of Bolu plain, as seen in the other basins along the NAFZ (Yoshioka 1996; Gürbüz & Gürer 2009).

Although we determined faults in the Bolu plain by using seismic reflection studies, different interpretations are also possible. For example, the Kasaplar and Bürnük faults can be interpreted as a single fault line passing through to the north of Hisar Tepe. An additional seismic line on the SW of Hisar Tepe is necessary to eliminate this possibility in future studies. Another option lies on the SE continuation of the Dağkent Fault. Even if our Line-6 (Figs 5 and 12) demonstrates that the prolongation of the Dağkent Fault does not exist here, further seismic studies are necessary on the NE extension of Line-6 to be sure about this evaluation. In the east of Bolu city centre, additional seismic lines are also required to determine the exact location of the bending of the Dağkent Fault. Nevertheless, these weaknesses do not affect the fact that the northern branch of the NAFZ is connected to the main branch via the Bolu plain, that is the best candidate for a future earthquake location and also indicates that the pull-apart nature of the Bolu plain has been terminated.

6. CONCLUSIONS

This paper determines the non-ruptured missing link between the Bakacak Fault and the main branch of the North Anatolian Fault Zone that constitutes the NE part of the Almacık block. The Kasaplar and Bürnük faults were followed clearly in the seismic reflection studies and they are seismically active faults as proven by recent earthquake focal mechanism solutions (Table 1). They should be taken into account in the evaluation of seismic risk assessment for the Bolu city centre. These newly recognized active faults in the Bolu plain are equally important as the next envisaged seismic event following the 1999 earthquakes in the Marmara Sea because it is demonstrated that, after a strike-slip related earthquake, the stress accumulation occurs at the both ends of a fault rupture (Stein *et al.* 1997). The Kasaplar, Dağkent and Bürnük faults determined in this paper are located on the eastern end of the 1999 earthquake surface ruptures along North Anatolian Fault Zone, and for the reasons given above they are the best candidates for the production of future earthquakes in the region.

ACKNOWLEDGEMENTS

This paper is part of a project MARKA 11–02-DFD-174 supported by Bolu Provincial Administration, EU Projects and External Relations Coordinatorship, the Turkish Republic East Marmara Development Agency. Additional field studies were supported by

Downloaded from https://academic.oup.com/gji/article/201/3/1814/754781 by ANKARA user on 12 December 2021

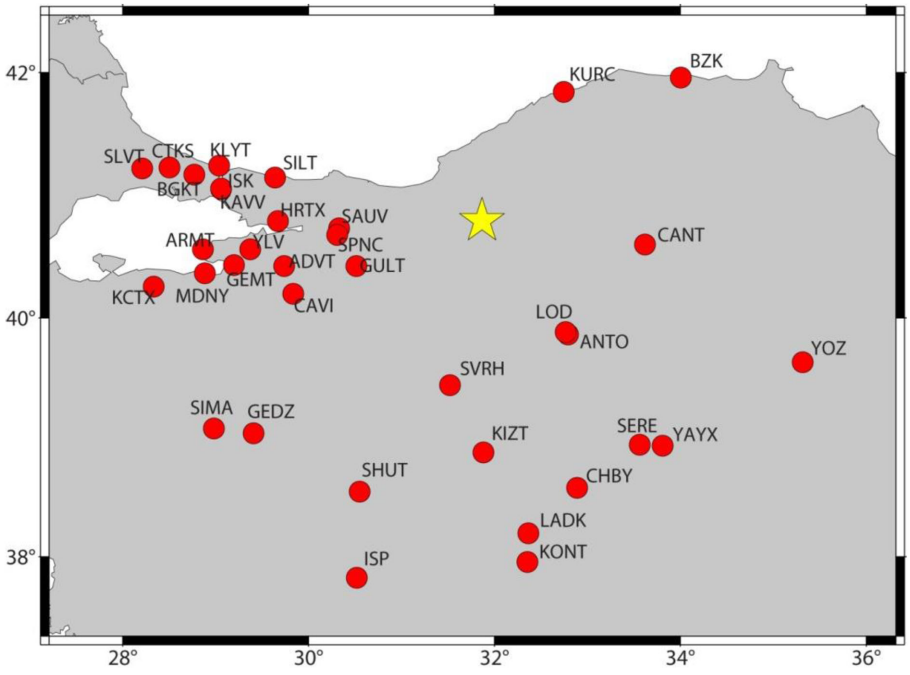


Figure 17. Location of KOERI broadband station distribution (solid circles) used for moment tensor inversion analysis of the2013 November 24 earthquake (UTC 20:49:38; $M_L = 5.0$) indicated with a star.

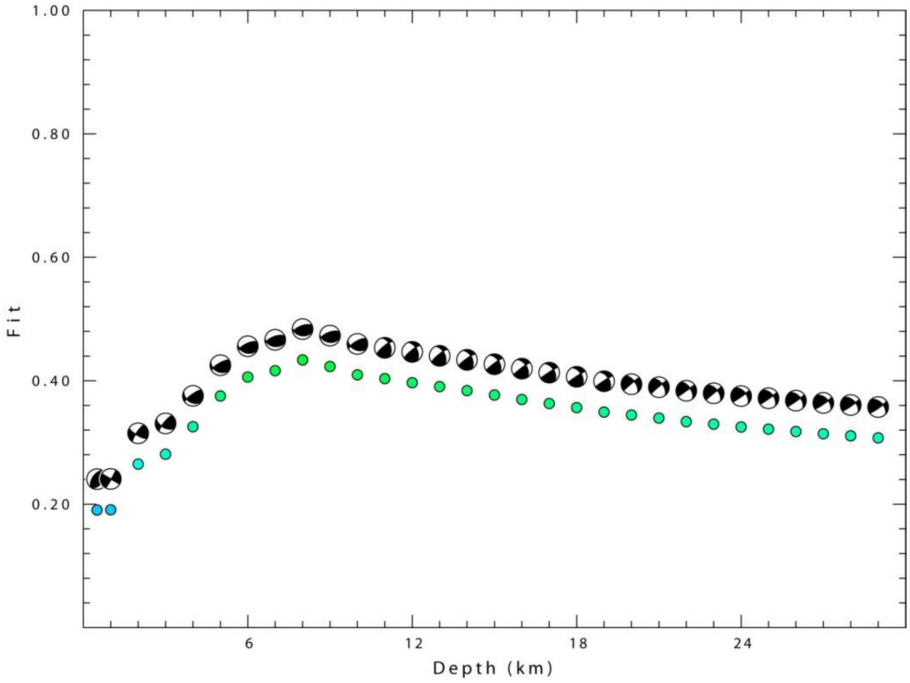


Figure 18. Correlation plot of the reduction in distance-weighted variance against source depth for the earthquake of 2013 November 24, 20:49:38 (UTC). The best fit is provided for a depth of 8 km.

TUBİTAK project no. 111Y227. We also thank Yüksel Karabulut for his great help and organisation skills during the seismic studies. For the seismological earthquake data we are grateful to the KOERI - Boğaziçi University, Kandilli Observatory and Earthquake Research Institute. The editorial handling by Egill Hauksson and valuable comments of two anonymous reviewers have improved an earlier version of this manuscript, for which we are grateful.

Downloaded from https://academic.oup.com/gji/article/201/3/1814/754781 by ANKARA user on 12 December 2021

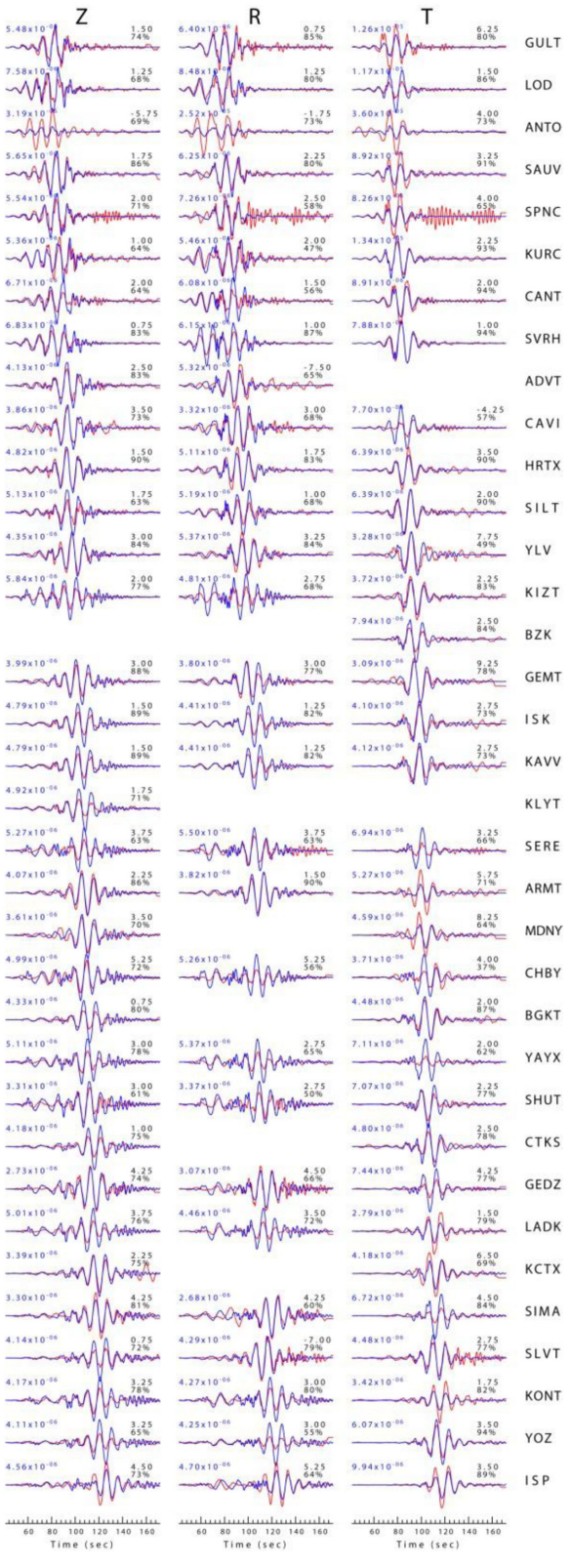


Figure 19. Overlaid observed (red—light gray) and predicted (blue—dark gray) waveforms for the earthquake of 2013 November 24, 20:49:38 (UTC). Each observed-predicted component is plotted to the same scale and peak amplitudes are indicated by the numbers to the left of each trace. The values of time shift and percentage of variance reduction are given as upper and lower numbers on the right of each trace. The station names are given to the right of the traces.

REFERENCES

Aktimur, H.T., Ateş, S. & Oral, A., 1986. Seismic zonation in the vicinity of Bolu for the earthquake hazard minimization, *Tür. Jeol. Kur. Bült.,* **29,** 43–49. (in Turkish)

Alpar, B. & Yaltırak, C., 2002. Characteristic features of the North Anatolian Fault in the eastern Marmara region and its tectonic evolution, *Mar. Geol.,* **190,** 329–350.

Angelier, J., 1990. Inversion of field data in fault tectonics to obtain the regional stress III: a new rapid direct inversion method by analytical means, *Geophys. J. Int.,* **103,** 363–376.

Arca, M.S., 2004. Neotectonics and evolution of the Yeniçağa basin, Bolu, Turkey, *MSc thesis,* METU.

Armijo, R., Meyer, B., Navarro, S., King, G. & Barka, A., 2002. Asymmetric slip partitioning in the Sea of Marmara pull-apart: a clue to propagation processes of the North Anatolian Fault?, *TerraNova,* **14,** 80–86.

Ayhan, M.E. & Koçyiğit, A., 2010. Displacements and kinematics of the February 1, 1944 Gerede Earthquake (North Anatolian Fault System, Turkey): geodetic and geological constraints, *Turkish J. Earth Sci.,* **19,** 285–311.

Barka, A., 1992. The North Anatolian fault zone, *Ann. Tect.,* **6,** 164–195.

Barka, A. & Kadinsky-Cade, K., 1988. Strike-slip fault geometry in Turkey and its influence on earthquake activity, *Tectonics,* **7,** 663–684.

Barka, A.A. & Kuşçu, İ., 1996. Extents of the North Anatolian fault in the İzmit, Gemlik and Bandırma bays, *Turkish J. Marine Sci.,* **2,** 93–106.

Başokur, A., Gökten, E., Seyitoğlu, G., Ulugergerli, E., Kadıoğlu, S., Özaksoy, V. & Arman, N., 2004. *Dating the historical events of the North Anatolian fault in the Bolu Basin by trench studies and locating of the exact place of the North Anatolian fault by GPR measurements,* Ankara University Research Foundation Project Report 2001.07.05.058. (in Turkish)

Bécel, A., Laigle, M., de Voogd, B., Hirn, A., Taymaz, T., Yolsal-Çevikbilen, S. & Shimamura, H., 2010. North Marmara Trough architecture of basin infill, basement and faults, from PSDM reflection and OBS refraction seismics, *Tectonophysics,* **490,** 1–14.

Bekler, T. & Gürbüz, C., 2008. Insight Into the crustal structure of the Eastern Marmara Region, Nw Turkey, *Pure appl. Geophys.,* **165,** 295–309,

Çakır, Z., Barka, A.A., De Chabalier, J.-B., Armijo, R. & Meyer, B., 2003. Kinematics of the November 12, 1999 (M_w = 7.2) Düzce earthquake deduced from SAR Interferometry, *Turkish J. Earth Sci.,* **12,** 105–118.

Dolu, E. *et al.*, 2007. Quaternary evolution of the Gulf of İzmit (NW Turkey): a sedimentary basin under control of the North Anatolian Fault Zone, *Geo-Mar. Lett.,* **27,** 355–381.

Emre, Ö., Duman, T.Y. & Özalp, S., 2011. Bolu (NK 36–14) quadrangle. 1:250 000 scale active fault map series of Turkey, serial number 19, General Directorate of Mineral Research and Exploration.

Emre, Ö., Erkal, T., Kazancı, N., Görmüş, S., Görür, N., Kuşçu, İ. & Keçer, M., 1997. Morphotectonics of the southern Marmara region during the Neogene and Quaternary, in *The Neogene and Quaternary evolution of southern Marmara region,* pp. 36–68, eds. Kazancı, N. & Görür, N., Tübitak Project Report YDABÇAG-426/G. (in Turkish)

Gökten, E., Demirtaş, R., Özaksoy, V., Herece, E., Varol, B. & Temiz, U., 2011. Faulting and stress distribution in the Bolu Pull-apart Basin (North Anatolian Fault Zone, Turkey): the significance of new dates obtained from the Basin Fill, *Turkish J. Earth Sci.,* **20,** 1–26.

Gündoğdu, O., 2010. Earthquake risk in Bolu and surroundings, in *National Earthquake Symposium,* 11–12 November 2009, pp. 37–44, Abant İzzet Baysal University. (in Turkish)

Gürbüz, A. & Gürer, Ö.F., 2008. Tectonic Geomorphology of the North Anatolian Fault Zone in the Lake Sapanca Basin (Eastern Marmara Region, Turkey), *Geosci. J.,* **12,** 215–225.

Gürbüz, A. & Gürer, Ö.F., 2009. Middle Pleistocene extinction process of pull-apart basins along the North Anatolian Fault Zone, *Phys. Earth planet. Inter.,* **173,** 177–180.

Herece, E., 2005. Neotectonic features of the western part of the North Anatolian Fault Zone, *PhD thesis,* Ankara University.

Downloaded from https://academic.oup.com/gji/article/201/3/1814/754781 by ANKARA user on 12 December 2021

Herece, E. & Akay, E., 2003. *Atlas of North Anatolian Fault,* Special Publication Series-2, pp. 61, General Directorate of Mineral Research and Exploration, ISBN:975-6595-54-X.

Herrmann, R.B., Benz, H. & Ammon, C.J., 2011. Monitoring the earthquake source process in North America, *Bull. seism Soc. Am.,* **101,** 2609–2625.

Hisarlı, Z.M., Cengiz Çinku, M. & Orbay, N., 2011. Paleomagnetic evidence of complex tectonic rotation pattern in the NW Anatolian region: implications for the tectonic history since the Middle Eocene, *Tectonophysics,* **505,** 86–99.

Hitchcock, C., Altunel, E., Barka, A.A., Bachhuber, J., Lettis, W., Kozacı, Ö., Helms, J. & Lindvall, S., 2003. Timing of Late Holocene earthquakes on the eastern Düzce Fault and implications for slip transfer between the southern and northern strands of the North Anatolian Fault System, Bolu, Turkey, *Turkish J. Earth Sci.,* **12,** 119–136.

İşseven, T., Demir, T., Genç, Ş.C. & Gülmez, F., 2009. How has strike slip motion on the North Anatolian Fault rotated the Almacık block?, in *62nd Geological Congress of Turkey Abstracts Book,* pp. 936–937, Chamber of Geological Engineers of Turkey.

Klein, F.W., 2002. User's guide to HYPOINVERSE-2000, a fortran program to solve for earthquake locations and magnitudes, Geological Surv. Open-File Report 2002–171.

Koçyiğit, A., 1988. Tectonic setting of the Geyve basin: Age and total displacement of the Geyve Fault Zone, *METU J. Pure Appl. Sci.,* **21,** 81–104.

Kurtuluş, C. & Canbay, M.M., 2007. Tracing the middle strand of the North Anatolian Fault Zone through the southern Sea of Marmara based on seismic reflection studies, *Geo-Mar. Lett.,* **27,** 27–40.

Michel, G.W., Faldhor, M., Neugebauer, J. & Appel, E., 1995. Sequential rotation of stretching axes, and block rotations, a structural and paleomagnetic study along the North Anatolian Fault, *Tectonophysics,* **243,** 97–118.

Neugebauer, J., 1995. Structures and kinematics of the North Anatolian Fault zone, Adapazarı-Bolu region, northwest Turkey, *Tectonophysics,* **243,** 119–134.

Okay, A.I., Demirbağ, E., Kurt, H., Okay, N. & Kuşçu, İ., 1999. An active, deep marine strike-slip basin along the North Anatolian fault in Turkey, *Tectonics,* **18,** 129–147.

Özden, S., Över, S., Kavak, K.S. & İnal, S.S., 2008. Late Cenozoic stress states around the Bolu Basin along the North Anatolian Fault, NW Turkey, *J. Geodyn.,* **46,** 48–62.

Öztürk, A., İnan, S. & Tutkun, S.Z., 1985. Tectonics of Abant-Yeniçağa (Bolu) region, *Cum. Üniv. Müh. Fak. Derg.,* **2,** 33–50. (in Turkish)

Öztürk, K., Yaltırak, C. & Alpar, B., 2009. The relationship between the tectonic setting of the lake İznik basin and the middle strand of the North Anatolian Fault, *Turkish J. Earth Sci.,* **18,** 209–224.

Sarıbudak, M., Sanver, M., Şengör, A.M.C. & Görür, N., 1990. Paleomagnetic evidence for substantial rotation of the Almacık block within the Anatolian Fault Zone, NW Turkey, *Geophys. J. Int.,* **102,** 563–568.

Sasvári, Á. & Baharev, A., 2014. SG2PS (Structural Geology to Postscript Converter) – A graphical solution for brittle structural data evaluation and paleostress calculation, *Comput. Geosci.-UK,* **66,** 81–93.

Selim, H.H., Tüysüz, O. & Barka, A.A., 2006. Neotectonics of the south Marmara subregion, *İTÜ Derg.,* **5,** 151–160.

Şengör, A.M.C., 1979. The North Anatolian transform fault: its age, offset and tectonic significance, *J. Geol. Soc. Lond.,* **136,** 269–282.

Şengör, A.M.C., Görür, N. & Şaroğlu, F., 1985. Strike-slip faulting and related basin formation in zones of tectonic escape: Turkey as a case study, in *Strike-Slip Faulting and Basin Formation,* Vol. 37, pp. 227–264, eds. Biddle, K.T. & Christie-Blick, N., Soc Econ Paleont Miner, Spec Publ.

Şengör, A.M.C., Tüysüz, O., İmren, C., Sakınç, M., Eyidoğan, H., Görür, N., Le Pichon, X. & Rangin, C., 2005. The North Anatolian Fault: a new look, *Ann. Rev. Earth Planet Sci.,* **33,** 37–112.

Seyitoğlu, G., 1984. Geology of Southern Sünnice mountain, *MSc thesis,* İstanbul Teknik Üniversitesi. (in Turkish)

Seyitoğlu, G., 2000. Is there an earthquake risk around the Bolu?, *Cum. Bil. Tek.,* **696,** 20–21. (in Turkish)

Stein, R.S., Barka, A.A. & Dieterich, J.A., 1997. Progressive failure on the North Anatolian Fault since 1939 by earthquake stress triggering, *Geophys. J. Int.,* **128,** 594–604.

Tur, H., Ecevitoğlu, B. & Şimşek, M., 2000. Shallow seismic imaging of South Marmara, in *Geophysical Conference on South Marmara Earthquakes,* September 28, pp. 53–55, Tayyare Cultural Center. (in Turkish)

Widess, M.B., 1973. How thin is a thin bed, *Geophysics,* **38,** 1176–1180.

Yaltırak, C., 2002. Tectonic evolution of the Marmara Sea and its surroundings, *Mar. Geol.,* **190,** 493–529.

Yılmaz, M. & Koral, H., 2007. Neotectonic features and geological development of the Yenişehir basin (Bursa), *İst Yerbilimleri,* **20,** 21–32. (in Turkish)

Yoshioka, T., 1996. Evolution of fault geometry and development of strike-slip basins: comparative studies on the transform zones in Turkey and Japan, *Island Arc.,* **5,** 407–419.

Downloaded from https://academic.oup.com/gji/article/201/3/1814/754781 by ANKARA user on 12 December 2021